Submitted to: Review of Scientific Instruments

Design and Operation of a Scanning Electrochemical Microscope for Imaging with Continuous Line Probes

Anna E. Dorfi,[1] Han-wen Kuo,[2] Vera Smirnova[1], John Wright,[2*] and Daniel V. Esposito[1*]

[1] Department of Chemical Engineering, Columbia Electrochemical Energy Center, Lenfest Center for Sustainable Energy, Columbia University in the City of New York, New York, NY 10027, USA
[2] Department of Electrical Engineering, Data Science Institute, Columbia University in the City of New York, New York, NY 10027, USA

[*]Correspondence to: de2300@columbia.edu; jw2966@columbia.edu

Abstract

This article describes a home-built scanning electrochemical microscope capable of achieving high areal imaging rates through the use of continuous line probes (CLPs) and compressed sensing (CS) image reconstruction. The CLP is a non-local probe consisting of a band electrode, where the achievable spatial resolution is set by the thickness of the band and the achievable imaging rate is largely determined by its width. A combination of linear and rotational motors allows for CLP scanning at different angles over areas up to 25 cm^2 to generate the raw signal necessary to reconstruct the desired electrochemical image using CS signal analysis algorithms. Herein, we provide detailed descriptions of CLP fabrication, microscope design, and procedures used to carry out SECM imaging with CLPs. In order to illustrate the basic operating procedures for the microscope, line scans and images measured in substrate generation-probe-collection mode for flat samples containing platinum disc electrodes are presented. These exemplary measurements illustrate methods for calibrating the positioning system, positioning and cleaning the CLP, and verifying proper positioning/probe sensitivity along its length.

Key words: Scanning electrochemical microscopy (SECM), scanning probe microscopy (SPM), compressed sensing, band electrode.

I. Introduction

Scanning electrochemical microscopy (SECM) is a powerful scanning probe microscopy (SPM) imaging method used for evaluating the chemical and physical properties of materials at microscopic and nanoscopic length scales.[1–5] The vast majority of SECM measurements performed to date have used conventional ultramicroelectrode (UME) probes, which typically consist of a metallic wire sealed in an insulating glass sheath. During operation, the electrochemical interaction between this UME "point probe" and the sample are recorded in a point-by-point sensing scheme as the UME is scanned across an area of interest. A major shortcoming of conventional point probes is that they require very long scan times to image large sample areas with high resolution.[6,7] In general, long scan times result in low throughput and can lead to unwanted changes in the sample or probe.

Previous research efforts have attempted to overcome the trade-off between resolution and areal imaging rates through a variety of approaches that have involved modifications to SECM hardware[1,8–12], the use of advanced probe geometries[13–16], and/or post measurement image processing to correct for blurriness and artifacts associated with fast scan speeds.[13,15–18] For example, the development of scanning droplet cells for scanning electrochemical cell microscopy (SECCM), combined with the use of more efficient spiral scan patterns, has resulted in substantial increases in areal imaging rates thanks to their ability to utilize high scan rates without being limited by convection.[2,3,19–21] Alongside instrument development, the use of innovative probe configurations and geometries has emerged as a promising approach to increase SECM imaging rates.[13,14,22–24] For example, multiple studies have demonstrated the use of individually addressable sub micrometer electrodes for large area imaging.[13,15] Lesch et. al combined the idea of using a linear array of microelectrodes with polymeric thin films to create

soft, flexible probes capable of imaging large sample areas, even for tilted and curved surfaces.[13,14,25] Yet, the resolution of these probes remains limited by the lateral spacing between the point probes embedded within the array. Additionally, fabrication of these probes is non-trivial, and more complex electronics (e.g. multiplexer or multichannel potentiostat) are required to analyze the signals from the individually addressable electroactive elements.

Recently, we have demonstrated an alternate approach to increasing SECM imaging rates by using a continuous line probe (CLP) consisting of a high aspect ratio band electrode sealed between two insulating sheets.[22] In principle, the CLP can achieve high imaging rates by sensing probe/substrate interactions everywhere along its length, while simultaneously achieving high spatial resolution that is set by the thickness of the band electrode. By performing multiple CLP scans across a region of interest at different substrate scan angles, sufficient information can be obtained to reconstruct a 2D SECM image. A complication of SECM imaging with a CLP (CLP-SECM) is that the nonlocal nature of the CLP requires advanced signal analysis methods to reconstruct images from the convoluted information contained in the raw CLP scans. Fortunately, this task can be efficiently achieved using modern compressed sensing (CS) reconstruction methods.[17,18]

Our previous study described the basic principles of CLP-SECM imaging with CS image reconstruction, but the quality and areal imaging rates demonstrated in that work were limited by the CLPs and microscope set-up employed in that study.[22] Specifically, those first demonstrations involved tedious probe positioning, sample rotation, probe cleaning, and data acquisition procedures that increased imaging times and introduced unnecessary human error into the measurement scheme. In the current paper, we describe a custom-built programmable scanning electrochemical microscope setup for CLP-SECM imaging that can overcome these

limitations. The advantages of this new instrument include is its ability to perform programmable rotational movements with simple hardware and probe design, allowing for streamlined data acquisition of electrochemical data. Herein, we first describe the procedures for fabricating and characterizing the CLP used in this study before detailing the system design and key microscope components. Subsequently, the communication and control of the hardware is explained and example measurements from the instrument are presented.

II. Design and operating principles of CLP-SECM

2.1 Microscope design and operation

Figure 1 contains a simple block diagram showing the key components of our microscope and how they are configured with respect to each other. The overall design and many of the key components of this microscope share many similarities with conventional SECM instruments, which have been described in detail in previous publications.[5,26,27] Common SECM components include X, Y, and Z positioners for precise control over the probe position and a bipotentiostat to control the applied potential of the probe and substrate. A key difference is that the SECM instrument is specially designed to carry out imaging with continuous line probes (CLPs) thanks to integration of a programmable, high precision rotational positioner that rotates the sample stage in between line scan measurements. The rotational positioner is stacked on top of linear encoded programmable X and Y positioners, which collectively form the sample stage. An electrochemical cell containing the sample to be imaged is mounted on top of this stage and viewed from above by a CCD camera. A programmable Z positioner, independently secured to the microscope platform, possesses a mounting bracket for the CLP and serves the purposing of raising and lowering the CLP with respect to the sample to be imaged. The X, Y, Z, and rotational (R) positioners are connected to a common controller/power supply unit. The CCD

camera, positioner electronics, and bipotentiostat all interface with a personal computer (PC). In the following subsections (2.1.1-2.1.3), more details are provided about the design and characteristics of CLPs, the electrochemical cell, and positioning system.

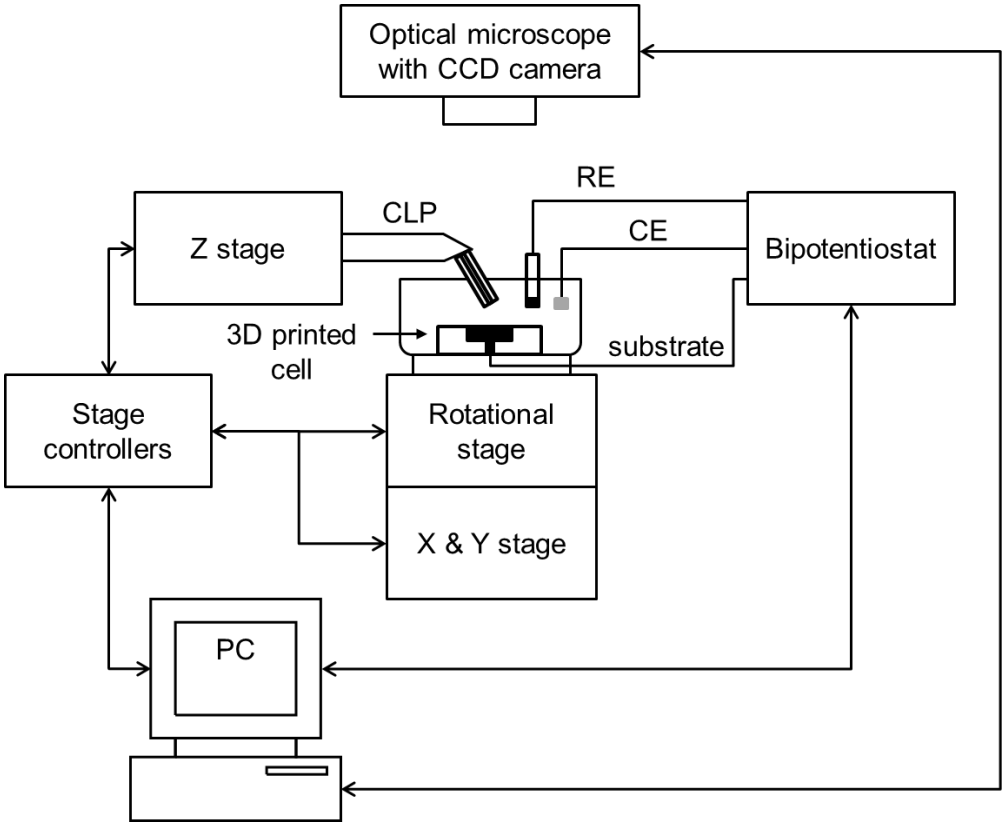

Figure 1. A schematic of the scanning electrochemical microscope setup with rotational and linear programmable motors for use with a continuous line probe (CLP).

2.1.1 Continuous line probes (CLPs)

A CLP is typically comprised of three layers: an insulating substrate, an electroactive layer, and a thin insulating layer.[22] As shown in Figure 2a, the electroactive sensing element is sandwiched between the two insulating layers. The thicker of the two insulating layers serves as the probe substrate support, while the thinner insulating layer serves as a spacer between the electroactive

layer and the sample during imaging. During imaging, the CLP is mounted onto a probe holder attached to the Z-positioner and positioned such that the thinner insulating layer comes in contact with the sample to be imaged (Figure 2b). The thickness of the thin insulating layer, t_I, combined with the CLP mounting angle with respect to the sample θ_{CLP}, determine the average separation distance between the sample and the electroactive layer (Figure 2b, inset). This average separation thickness d_m is calculated using Equation (1):

$$\mathrm{d_m} = \left(\frac{t_E}{2} + t_I\right)\sin(90° - \theta_{CLP}) \qquad \textbf{(1)}$$

In general, t_I should be similar to the thickness of the electroactive layer t_E in order to ensure that significant positive/negative feedback will be observed during SECM imaging with the CLP.

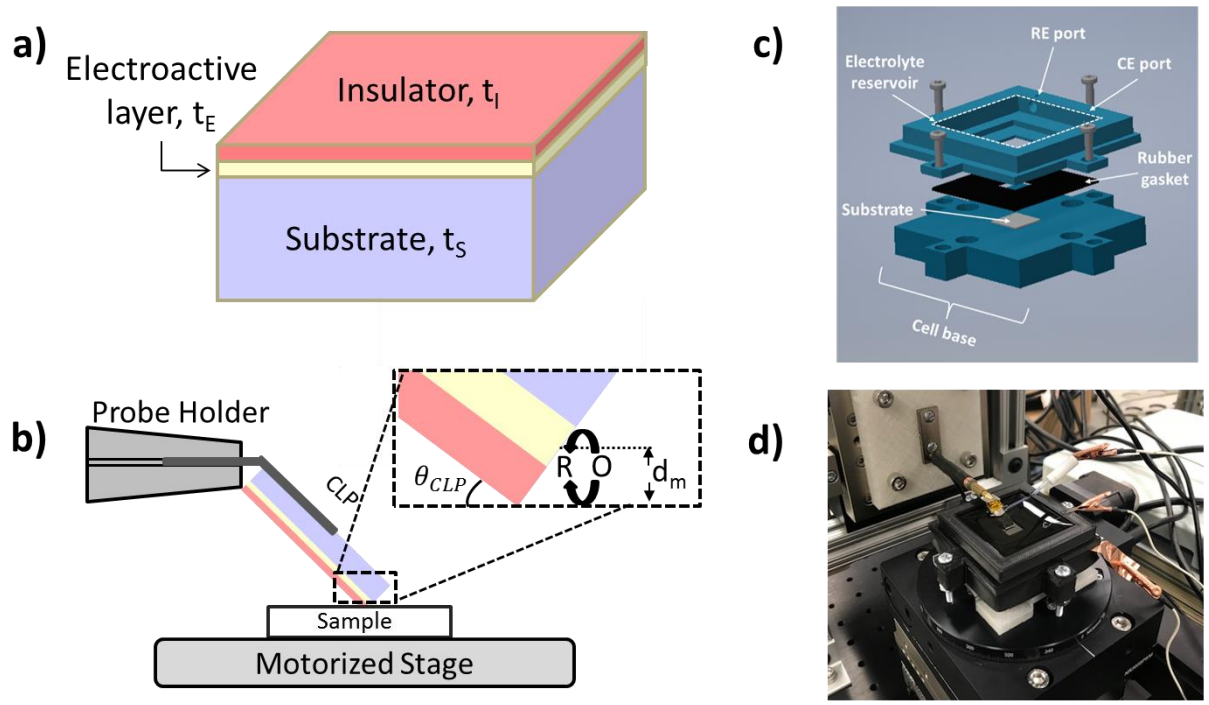

Figure 2 a.) A schematic 3D view of the different layers of a continuous line probe (CLP), including the insulating top layer, the electroactive layer, and the substrate layer. Layer thicknesses are not drawn to scale. b.) Schematic side-view of a CLP mounted on a probe holder and placed in contact with the sample to be imaged. Inset shows a close-up of the point of contact between the CLP and sample. c.) Exploded-view computer aided design (CAD) drawing of the custom electrochemical cell used in this study. d.) Photograph of the electrochemical cell mounted on the motorized positioning stage with CLP positioned in electrolyte for imaging.

2.1.2 Electrochemical cell

SECM measurements were performed in a custom low-profile cell that was designed in engineering design software and made from polylactic acid (PLA) using a 3D printer (MakerGear M3-ID). The computer aided design (CAD) files for this cell have been made freely available on the website echem.io, and a 3D rendering can be seen in Figure 2c. The cell consists of a base that connects directly to the rotational stage, and a top frame component that holds the electrolyte and attaches to the base. When assembling the cell, the sample to be imaged is clamped between the cell base and the frame using bolts and a rectangular rubber gasket to form a liquid-tight seal between the sample and the frame, while securely fastening all components to the rotational stage. The front side of the sample is exposed to the electrolyte through a square hole in the bottom of the upper frame component of the cell. Figure 2d contains a photograph showing the fully assembled cell mounted on the microscope stage during SECM measurements.

2.1.3 Linear and rotational positioners

The X, Y, and Z translational positioners can travel a maximum distance of 50 mm at a maximum velocity of 20 mm s^{-1}. The X and Y programmable positioners (Thorlabs, LNR50SE/M) are optically encoded and can achieve a minimum repeatable positional accuracy of 0.1 μm. The Z positioner (Thorlabs, LNR50S/M) possesses the same specifications as the X and Y stages except that it is not equipped with an optical encoder, having a minimum repeatable positional accuracy of 1 μm. The lower Z-position accuracy is permissible for CLP-SECM imaging since imaging occurs with the CLP in direct contact with the sample such that slight overshoot of the Z-position of the CLP has very little impact on the average probe/substrate separation distance. Rotation of the electrochemical cell is carried out using a rotational stage

(Thorlabs, NR360S/M) that travels 360° with a positional accuracy of 5 arcmin (≈.083°). As shown in Figure 1, the rotational, X, and Y positioners are stacked on top of each other to form the scanning stage upon which the electrochemical cell is mounted. Benchtop controllers (3 channels and 1 channel) are employed for controlling the positioners.

2.2 Communication and control schemes

The overall communication and control scheme for operation of the CLP-SECM is shown in the process control flow diagram provided in Figure 3. The control scheme was implemented through LabVIEW, which served as the user interface and platform to coordinate execution of user specified scanning conditions through the bipotentiostat and X, Y, Z, and rotational positioners. Beginning in the lower left corner of Figure 3, the operator must first enter the desired preconditioning and imaging parameters into the LabVIEW user interface. These include the applied potential for the probe and sample substrate, the coordinates of the center of the sample stage, the CLP scan rate, the scan distance, the probe Z position, the angular position of the substrate, and the total number of scans N. Next, the operator starts the imaging program, which successively executes the three sub-blocks labeled in Figure 3: i.) probe positioning and conditioning, ii.) execution of a single CLP scan, and iii.) repositioning of the CLP for the following scan. Upon completion of the N-th scan, the program ends and the recorded electrochemical data is used for post imaging processing and CS image reconstruction. In the following sub-sections, additional details are provided about the communication scheme, probe/substrate pretreatment, probe positioning algorithm, and post imaging data processing procedures that underlie the overall control scheme illustrated in Figure 3.

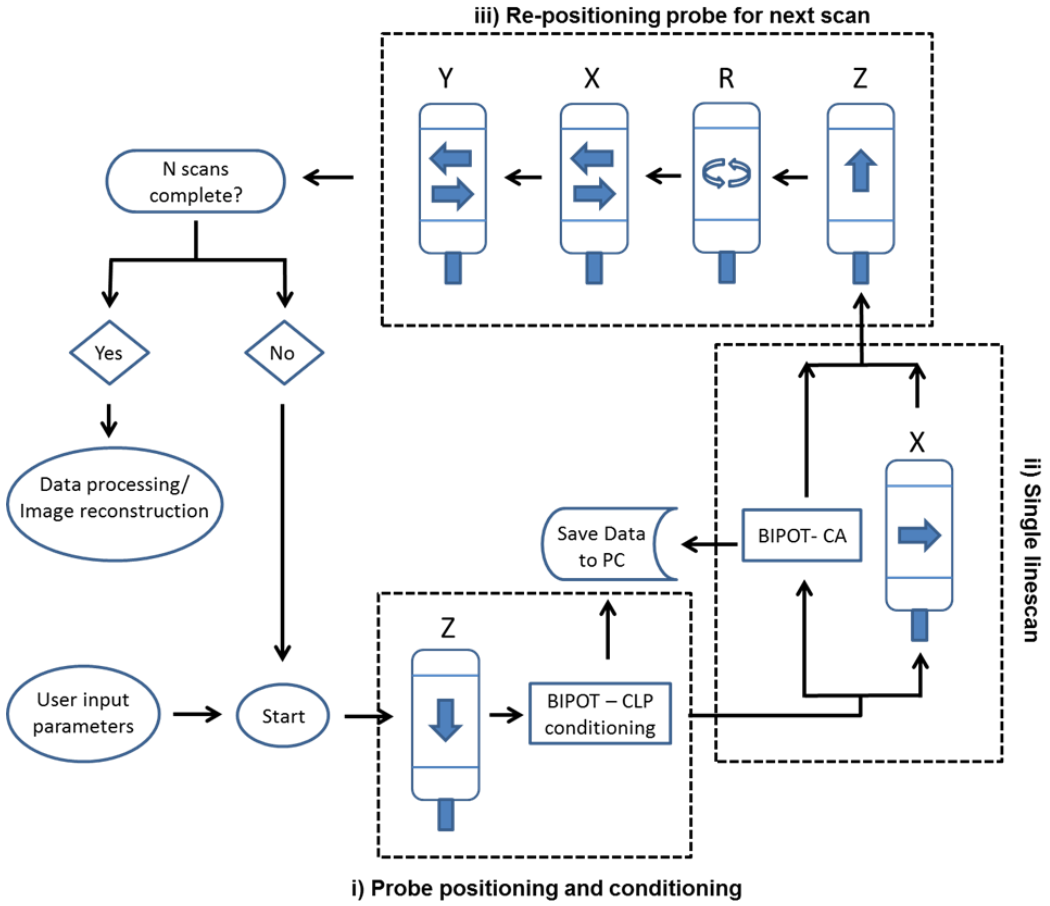

Figure 3. Process control flow diagram for CLP-SECM imaging. The blocks labeled X, Y, Z, and R represent the microscope positioners, and N represents the total number of scans.

2.2.1 Software and communication scheme

All positioners are controlled using the provided APT™ (Advanced Positioning Technology) software. Within the APT software, ActiveX Controls can be used within LabVIEW (NI LabVIEW 2017 32-bit) to control the positioners. The 700E CHI instruments, Inc. bipotentiostat used throughout this study comes with software that controls all potentiostat functions, and measures and records data. The CHI Instruments software also allows it to interface with LabVIEW, such that LabVIEW can be used to simultaneously control both the bipotentiostat and motorized stages. Within LabVIEW, programs are run through virtual instrument files (VI). The

LabVIEW user interface contains graphical representations of functions that are added as nodes and connected to control the flow and sequence of commands. The nodes are graphical objects in LabVIEW that have inputs and/or outputs and perform specific operations when a program runs. Within these objects, the operator specifies the aforementioned user inputs. The authors are happy to provide LABVIEW code upon request.

2.2.2 Electrode preconditioning and vertical positioning of CLP

Some preliminary positional inputs are necessary before a linescan can begin. These include positioning the sample to the desired start point and substrate scan angle using the X, Y, and rotational stages, as well as finding the vertical (Z position) needed for the line probe to be in contact with the substrate surface. The Z position is set by lowering the CLP with the vertical positioner until it comes in contact with the substrate surface. This distance for the Z position is then used as an input for the LabVIEW program. Similarly, the X, Y, and rotational positioners are all initially manually controlled to set the coordinates for the start of the scan. These coordinates are then also inputted into the LabVIEW program. Once all the necessary positional user inputs are set, the program begins with the vertical positioner lowering the CLP until it is in contact with the substrate. A cyclic voltammetry measurement of the probe surface while it is in contact with the sample surface is taken and the data is saved to the PC. Conditioning of the substrate with a cyclic voltammetry measurement is also done. This preconditioning step is done to “clean” both the probe and substrate surface by oxidizing organic matter that may be present and clearing the surface of any remaining reactant species from previous scans. The preconditioning step is important for maintaining a consistent background signal for all scans.

2.2.3 Execution of a single CLP linescan

Before a line scan is carried out, the sample stage must be positioned such that i.) the center of the sample area to be imaged is aligned with the midpoint of the CLP, ii.) the distance from the CLP midpoint to the center of the imaging area is set to half of the desired scan length, and iii.) the sample has the proper rotational orientation with respect to the X-scan direction such that the CLP scan will occur at the user-specified scan angle θ_S. After lowering the CLP using the Z-positioner, the line scan measurement begins by initiating potentiostatic control of the substrate and CLP potential, during the CLP and substrate currents are measured as a function of time. Current measured during these chronoamperometry (CA) measurements is recorded after an initial hold time, typically 240 s, which allows for dampening of transient signals from the CLP and/or substrate before imaging starts. Next, the CA data for the CLP is recorded and saved to the PC while the X-positioner is used to move the sample stage at the user specified step size and dwell time over the user specified scan distance.

2.2.4 Sample repositioning between successive scans

Once a line scan finishes, the Z-positioner lifts the CLP off the substrate and the sample stage must be repositioned for the next scan to be measured at a new scan angle θ_s. Figure 4a-c illustrates the procedure used for repositioning the sample stage between scans. After the stage is rotated (Figure 4b) by the user-specified angle θ_s with respect to the rotational center (x_r, y_r) along the X translational direction, the stage then translates in the X-Y plane with the probe position remaining fixed in the X-Y coordinate system. For every substrate position (x, y), its newly translated position $T(x, y)$ is calculated by assigning the location of the rotational center (x_r, y_r) of the stage and its rotational angle θ_s at the current scan, using the following Equation (2):

$$T(x,y) = \begin{pmatrix} cos\theta_s - 1 & sin\theta_s \\ -sin\theta_s & cos\theta_s - 1 \end{pmatrix} \begin{pmatrix} x_r \\ y_r \end{pmatrix} + \begin{pmatrix} x \\ y \end{pmatrix}, \quad \textbf{(2)}$$

The translation automatically relocates the substrate back to the scanning area A_{N+1}, which is equal to the initial scanning area A_1 (Figure 4c). The translation scheme allows us to perform a sequence of CLP scans without needing to position the stage rotational center right at the center of the substrate. This is important since the center of the area to be imaged can be located far from the axis of rotation for the rotational stage. The overall translation scheme is shown pictorially in Figure 4. Accurate translation of the stage between scans can be ensured as long as the i.) location of the rotation center of the stage (x_r, y_r) relative to the bottom end of the probe is known and ii.) all the reactive species reside within the inscribed circle of scanning area A_1. A more detailed description of this positioning algorithm is presented in section two of the supplementary information.

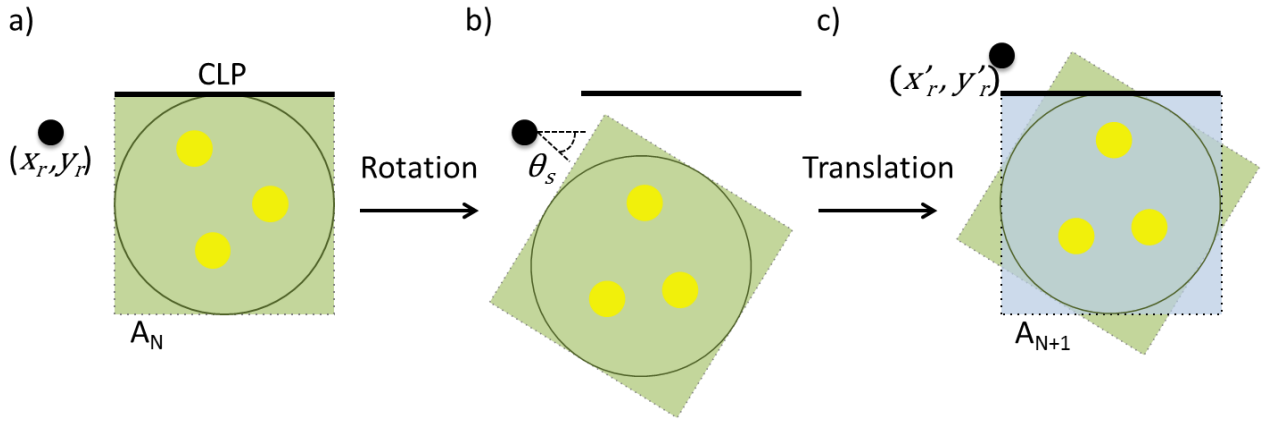

Figure 4. Schematic top views of CLP and hypothetical sample containing 3 electroactive discs illustrating how the sample orientation and positioning changes while rotating and translating the stage in between linescans of different scanning angles. a) The scanning area of the previous scan $\boldsymbol{A_N}$ is shaded in green, while the axis of rotation is located at $(\boldsymbol{x_r}, \boldsymbol{y_r})$ and marked with a dot. b.) View of the CLP and sample after the stage is rotated with respect to $(\boldsymbol{x_r}, \boldsymbol{y_r})$ by an angle θ_s. c.) View of the CLP and sample after translation of the sample stage by the X- and Y- motors , to a new position corresponding to the start location for the next scan. The scan area, $\boldsymbol{A_{N+1}}$, for the next scan is shaded grey, while the black circle marks the common area of analysis for both scan angles, which contains all of the electroactive objects of interest.

2.2.5 Post imaging data processing

Electrochemical data acquired by the bipotentiostat is saved as a technical data measurement (.tdm) file with a designated file name and location that is specified by the user at the beginning of the program run. The saved data can then be opened in a variety of programs (i.e. MATLAB, Excel) for post processing with compressed sensing (CS). As detailed in the supplementary information (SI) and our previous publication,[22] CS is used to reconstruct 2D SECM images from the current vs distance data acquired during each CLP scan. An abbreviated description of the CS reconstruction procedure used for the exemplary measurements included in this article is also included in the supplementary information.

III. Exemplary CLP-SECM measurements

3.1 Materials

All electrochemical measurements were carried out in aqueous solutions prepared from 18.2 MΩ-cm deionized water. Concentrated sulfuric acid (Certified ACS plus, Fischer Scientific), sodium sulfate (ACS reagent grade, Sigma Aldrich), potassium hexacyanoferrate(II) trihydrate (ACS reagent grade, Sigma Aldrich), sodium chloride (ACS reagent grade, Sigma Aldrich) were used as received without further purification. Platinum wire (Alfa Aesar, 99.95% metals basis, 50 μm diameter) served as the counterelectrode while a miniature Ag/AgCl electrode (EDAQ, 3 M KCl) was used as the reference electrode.

Fabrication of CLPs **–** Band microelectrodes were fabricated in a similar manner to what was described by Wehmeyer et al.[24] A Polycarbonate sheet (TapPlastics, 0.02 inch ≈500 μm thick), Pt foil (Alfa Aesar, 99.999% purity), and Kapton tape (1 Mil, 1⁄2" x 36 yds, Uline) were used as the materials of construction for the CLP. First, the 25 μm thick Pt foil (Fischer Scientific, 99.99% metals basis) was sealed to an insulating polycarbonate substrate using a two-part 5-minute epoxy (JB Weld). In order to ensure a good seal between the Pt and the PC substrate, a

vice was used to apply uniform pressure overnight while the epoxy cured. The top surface of the Pt foil was electrically insulated using Kapton tape (thickness ≈70 μm). The thickness of the Kapton tape is very important because it serves as the insulating layer that is in contact with the substrate during measurements, and therefore determined the average separation distance between the substrate and Pt layer. The CLP was cut to dimensions of 4.75 mm x 15 mm. The edge of the CLP was exposed by polishing with a home-built polishing system employing 1 μm alumina lapping paper (McMaster-Carr), followed by 0.3 μm alumina slurries. The end of the CLP was polished before measurements using a slurry of 0.05 μm Gamma alumina powder on a Microcloth polishing pad (CHI Instruments). Cyclic voltammetry (CV) characterization of the CLP in 1.4 mM potassium ferrocyanide (ACS Reagant grade, Sigma Aldrich) shows that the CLP exhibits diffusion controlled current at slow scan rates (Figure S1), with a limiting current consistent with that expected for a band electrode with t_E=25 μm.[26]

Fabrication of Ultramicroelectrodes (UMEs) **–** The UMEs used in this study were conventional disc-shaped ultramicroelectrodes made by sealing platinum wires in quartz glass capillaries using a laser-based pipette pulling procedure.[28,29] Platinum microwires (25 μm diameter, Alfa-Aesar) approximately 3 cm in length were attached to Cu leads (McMaster-Carr, 0.2 mm diameter) using silver epoxy (EpoTek H-22), and subsequently placed into quartz glass capillaries (Sutter Q100-50-10; OD 1 mm, I.D. 0.5 mm). The platinum was sealed in glass after connecting vacuum lines to the open ends of the capillary using Teflon tubing. Two stoppers were placed between the puller bars and the frame in order to minimize movement of the assembly with respect to the laser. A sealing program (heat: 660; fil: 5; vel: 60; del: 140; pul: 0) was run on average 5-7 times to seal the Pt in glass. After sealing, the stoppers and the vacuum lines were removed and a hard-pull was accomplished using the following program: heat: 875; fil: 2; vel: 120; del: 150; pul:

200. The UMEs were then checked under the microscope to ensure that there were no fractures in the platinum and then polished to 20 μm diameter with a home-built polishing station in order to expose the Pt disc.

Fabrication of substrates **-** The disc electrode patterns were prepared by evaporating metals (Ti as an adhesion layer and Pt as the electrocatalyst) onto degenerately doped p+Si wafers through a shadow mask via electron beam deposition (High Vacuum Angstrom EvoVac, $1x10^{-8}$ Torr base pressure). Titanium and Pt were deposited sequentially without having to break vacuum. The thicknesses of the Ti and Pt layers were set to 2 nm and 50 nm, respectively. Layer thickness was monitored during the deposition using a quartz crystal thickness monitor. Electrical connection to the back of the p+Si was made by use of silver (Ag) conductive paint (SPI supplies). When the substrate is clamped into the electrochemical cell for imaging, the sample back contact is physically pressed into a piece of copper foil tape (3M™ Copper Conductive Tapes) placed on the base of the cell. The electrical leads from the potentiostat cable are then attached to the Cu tape.

3.2 Evaluating uniformity of CLP sensitivity and probe/substrate separation distance

In order for SECM imaging with CLPs to be reliable and quantitative, it is essential to know if there is any variation in the sensitivity of the probe along its length. Non-uniform sensitivity along the length of the probe can arise from variation in i.) probe/substrate separation along the length of the probe and/or ii.) the intrinsic electrochemical properties in the active sensing element along its length. The sensitivity of the CLP as a function of probe length can be evaluated by scanning the CLP over a single, isolated electroactive object multiple times such that the object intersects the CLP scan path at different points along the probe. The point of intersection of the disc with the CLP sensing element can be characterized by its distance from

the center point of the CLP, *w*, as shown in the schematic top view of a CLP scan in Figure 5a. The CLP used in this study was characterized in an electrolyte of 1 mM H_2SO_4 in 0.1 M Na_2SO_4 by scanning it at 25 µm s^{-1} over an isolated 100 µm diameter Pt disc electrode for 13 different *w*. The measurement was carried out in substrate generation/probe collection mode, resulting in positive feedback from the H_2/H^+ redox reactions occurring between the disc electrode and sensing element of the probe.

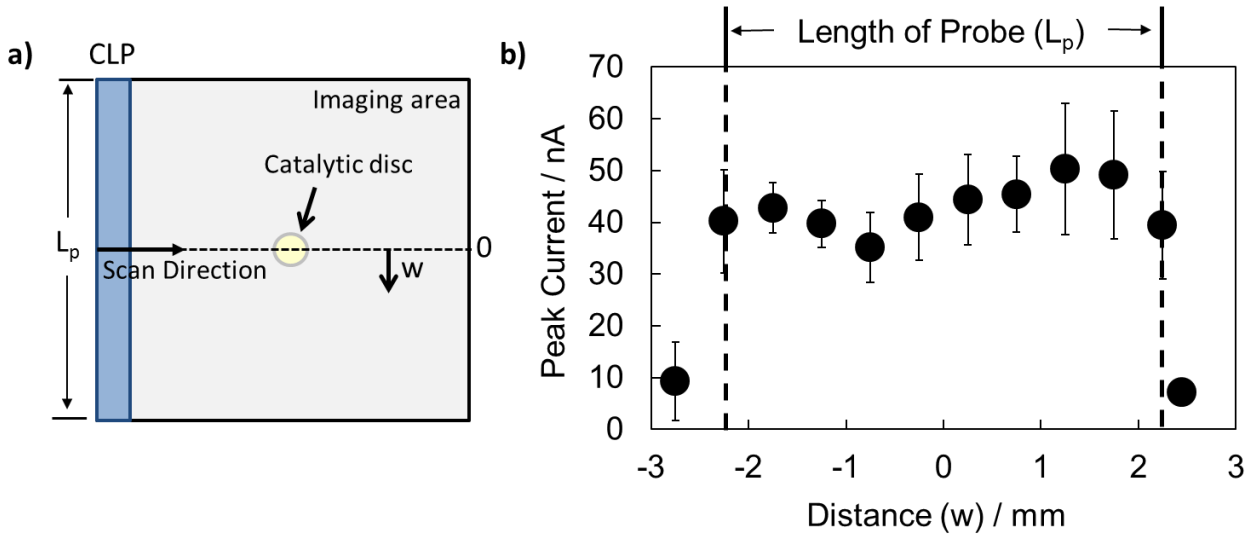

Figure 5. a) Schematic showing the characterization procedure of the CLP as it scans over a single electroactive disc with diameter of 100 µm at various locations along the length of the probe (w). b) Plot of the peak current measured from the CLP as a function of w. The error bars correspond to the 95% confidence interval for the average peak current density recorded during three different CLP scans at each location. The measurements were carried out in substrate generation probe collection mode in 1 mM H_2SO_4 in 0.1 M Na_2SO_4 at a scan rate of 25 µm s^{-1}. The CLP potential was held at 0.7 V vs Ag|AgCl and the sample was held at -0.8 V vs Ag|AgCl.

Using the peak current recorded by the probe during each scan as a proxy for the probe sensitivity, the probe sensitivity is plotted as a function of w in Figure 5b. For CLP scans characterized by *w* greater than half the length of the CLP ($L_p/2$), (*w*= -2.75 mm, +2.45 mm), negligible signal is recorded because the CLP scan path doesn't intersect the electroactive disc. When w < ($L_p/2$), significant peak current is observed, with an average signal of 37 $\pm$ 4 nA

recorded. Slight variations in probe sensitivity can be seen, including a minimum around w = -1 mm. Such non-uniformities might arise due to small inconsistencies in the cleanliness of the edge of the platinum foil sensing element, which might be caused by non-uniform polishing treatment and/or small amounts of residual organic matter that were not effectively removed during CV conditioning. Minor "edge effects", where the peak current is slightly reduced for $w \approx \pm (L_p/2)$, are also visible. A subtle increase in the recorded peak current with increasing w is also present, which can result from the end of the CLP not being perfectly parallel with the sample surface. The measurements in Figure 5b highlight the importance of taking great care to i.) fabricate well-defined CLP probes and ii.) position the CLP flush on the sample surface. Accurate CS-reconstruction of an SECM image does not require perfectly uniform sensitivity along the length of the CLP, but it is important to characterize non-uniformities in instances where significant variation in probe sensitivity exists. As we will detail in a future communication, CS reconstruction algorithms can use the probe sensitivity profile, such as that shown in Figure 5, to filter out artifacts of probe non-uniformities from the final reconstructed image.

3.3 Validating the CLP positioning algorithm

To validate the accuracy of the positioning algorithm described in SI section 2, CLP line scans were conducted over a single 250 μm diameter electroactive Pt disc (Figure 6) at four different scan angles, θ_s. The scans were recorded using the same conditions used for the CLP line scan measurements in Figure 5b, except that a slower scan rate of 10 μms^{-1} was employed. As desired, the CLP line scan profiles at each of the four scan angles overlay almost exactly (Figure 6b), confirming that our positioning algorithm accurately rotates and translates the stage in between scans such that the CLP and electroactive disc intersect each other at the midpoint of the scan.

This feature is not needed if the center of the imaging region of interest corresponds exactly to the rotational center of the stage but is critically important when those two points are not the same. Some slight variation in the peak current is seem for the four different CLP scan angles in Figure 6b, which might be explained by the small differences in sensitivity along the length of the probe that were shown in Figure 5b.

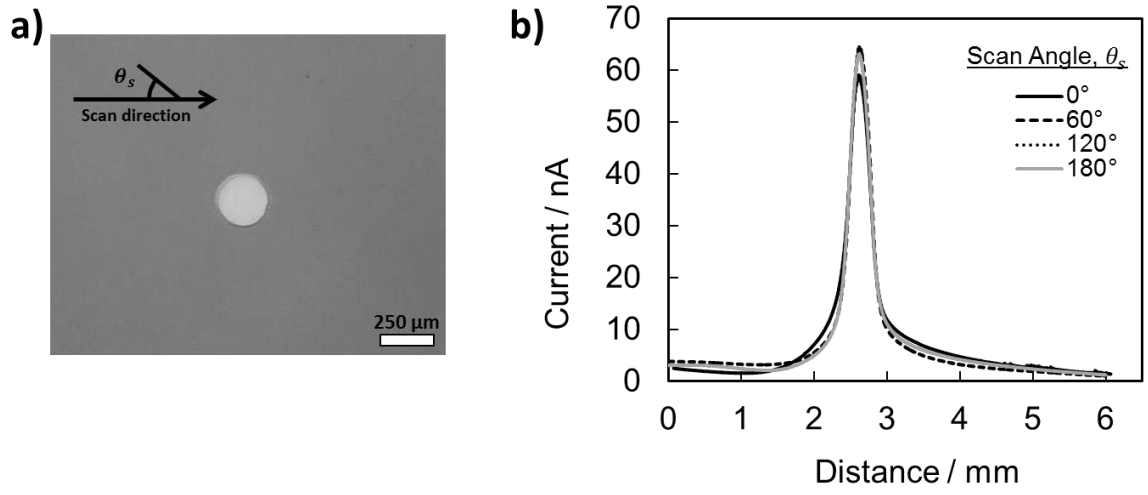

Figure 6. a) An optical image of a platinum disc with diameter of 250 µm. b) CLP line scans over the disc electrode in a.), recorded at varying scan angles at a step size of 10 µm s^{-1} in 1 mM H_2SO_4 and 0.1 M Na_2SO_4. The CLP potential was held at 0.7 V vs Ag|AgCl and the substrate was held at a mass transfer limiting potential for the hydrogen evolution reaction at -0.8 V vs Ag|AgCl.

3.4 Demonstration of CLP-SECM imaging

Having characterized the CLP sensitivity profile and validated the substrate positioning algorithm, a demonstration of CLP-SECM imaging was carried out using a sample containing three electroactive Pt discs with diameters of 150 µm (Figure 7a). Seven total CLP line scans were recorded sequentially using the process control scheme shown in Figure 3 and using the identical scan conditions described for the line scan measurements shown in Figure 6. The raw line scan signal for each of the scans is provided in Figure 7b. This data was then fed to

compressed sensing (CS) post processing code for image reconstruction to produce the 2D CLP-SECM image located in Figure 7c. A detailed description of the CS reconstruction algorithm can be found in our prior publication,[22] while details specific to its implementation in this work are provided in section three of the supplementary information.

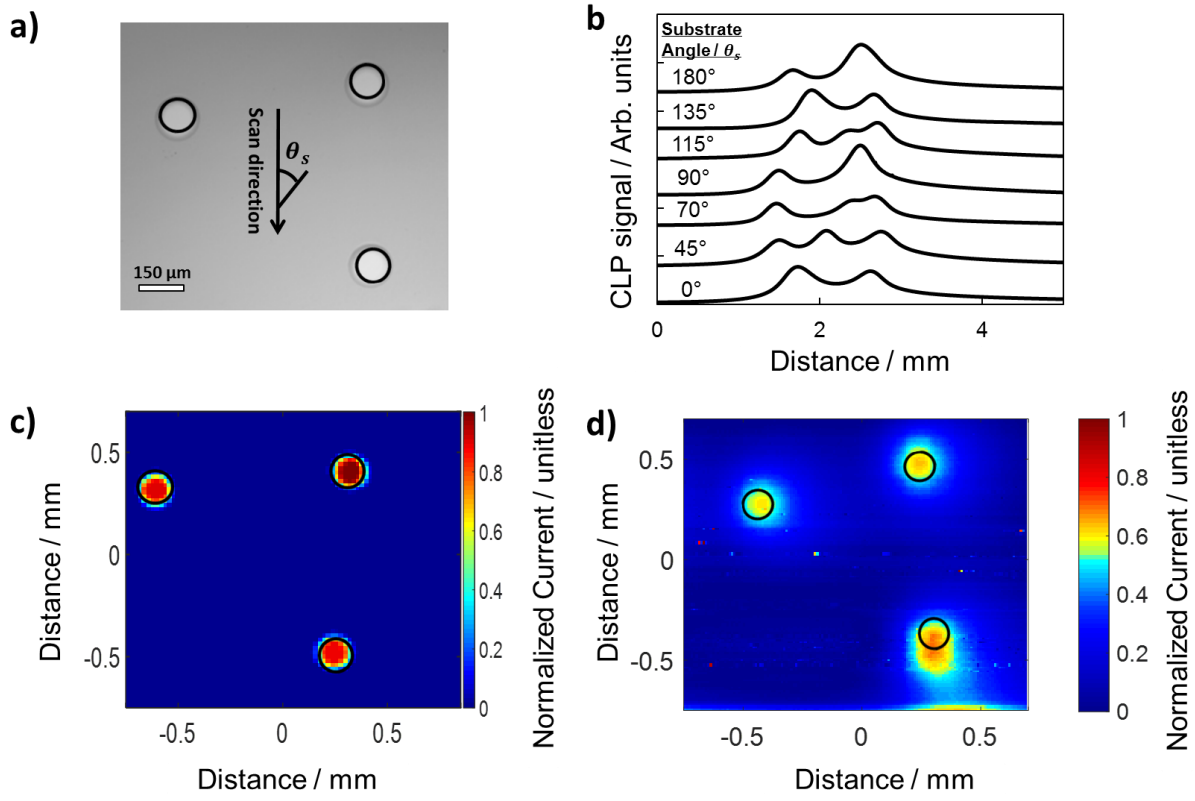

Figure 7. a.) Optical image of a sample consisting of three platinum discs deposited onto an inert p+Si substrate. The arrow that is superimposed on this image indicates the CLP scanning direction, while the stage is rotating clockwise by angle θ_s. b.) Individual CLP scans recorded for seven different sample rotation angles. c.) SECM image reconstructed from 4 of the linescans (0°, 45°, 70°, 135°) shown in panel b) using compressed sensing. d) SECM image generated by a conventional SECM instrument using a UME characterized by a probe diameter of ≈20 µm. All SECM measurements were carried out in substrate-generation, probe collection mode in a solution of 1 mM H_2SO_4 in 0.1 M Na_2SO_4 using a probe scan rate of 10 µm s^{-1}, a probe potential of 0.7 V vs Ag|AgCl, and a substrate potential of -0.8 V vs Ag|AgCl. The superimposed black circles in panels c.) and d.) are used to show the physical size and relative locations of the three Pt discs compared to the features recorded in SECM measurements. The conventional SECM image was recorded by scanning the probe from left to right, starting at the top of the sample area and working downwards in a raster pattern.

The CS-reconstructed CLP-SECM image in Figure 7c accurately displays three circular features having diameters and locations that is in good agreement with the location of the disc electrodes seen in Figure 7a. Four scans were used to generate the reconstructed image in Figure 7c, but as few as 3 scans were found to be sufficient to accurately determine that three-disc electrodes were present on the surface. Figure S4 in the Supplementary Information shows how the quality of the reconstructed image of the 3-disc sample changes when using 3, 4 5, and 6 linescans. As expected for identical disc electrodes, the three discs displayed in the reconstructed image all exhibit similar signal intensity. For comparison, SECM imaging of the same sample was carried out using a conventional UME with a commercial CHI 700E SECM instrument, with the result shown in Figure 7d. A ≈20 μm diameter Pt UME, similar to the thickness of the Pt foil used for the electroactive layer in the CLP (≈ 25 μm), was used for the conventional SECM measurement. Imaging with the UME was performed using a probe/substrate separation distance of 60 μm, identical to the average probe/substrate separation distance for the CLP when it is positioned at an angle of θ_{CLP} = 45° with respect to the substrate surface. In comparing the SECM images shown in Figure 7c and d, we find that the use of CLPs and UMEs with similar probe critical dimensions, probe/substrate separation distance, and identical scan rates (10 μm s^{-1}) results in SECM images of similar quality. However, there is some distortion in the point-probe SECM image at the end of the scan, most likely due to sample drift and/or changes in the electrochemical environment from evaporation of the electrolyte over the long measurement period. Although the conventional SECM image has similar quality than the CLP-SECM image, the former required ≈ 9 hrs. of imaging compared to the ≈ 1 hr. of scan time required to complete the 4 CLP linescans used to reconstruct the latter. It should also be noted that this large time advantage was achieved while scanning over a circular sample area that was roughly two

times larger than the rectangular area imaged by the UME. As detailed elsewhere,[22] the total imaging time required for imaging with non-local probes can be orders of magnitude less than a conventional UME for samples that are characterized by even larger ratios of the scan area dimension to the desired imaging resolution.

IV. Conclusions

This article has described the design, operating principles, and implementation of a programmable scanning electrochemical microscope that allows for high-throughput imaging with non-local continuous line probes. The key novelty of this instrument compared to commercial SECM instruments is that it possesses a programmable rotational sample stage that allows for automated imaging with a CLP at scan angles from 0° to 360°. In addition to describing the overall design and control scheme for the microscope, this article presented methods for CLP characterization and validation of the probe positioning algorithm. A side-by-side imaging comparison of CLP-SECM with conventional SECM was also carried out using a sample based on three Pt disc electrodes. This comparison shows that a CLP-SECM instrument is capable of generating CS-reconstructed SECM images with similar quality to those generated with a commercial SECM instrument using a conventional UME probe of similar critical dimension and probe/substrate separation distance. Overall, this result demonstrates the potential of SECM instruments employing non-local probes such as CLPs to drastically reduce SECM imaging rates compared to conventional SECMs based on UME "point probes".

V. Supplementary material

See supplementary material for more information on CLP characterization, the automated sample alignment procedure, and a more detailed description of CS and the image reconstruction algorithm.

VI. Acknowledgements

The authors would like to acknowledge funding support from the National Science Foundation under Grant Number (NSF CHE-1710400). Any opinions, findings, and conclusions or recommendations expressed in this material are those of the author(s) and do not necessarily reflect the views of the National Science Foundation. The authors would also like to acknowledge Adekunle David Balogun for help with fabricating electrochemical cell prototypes.

VII. References

[1] C.L. Bentley, J. Edmondson, G.N. Meloni, D. Perry, V. Shkirskiy, and P.R. Unwin, Anal. Chem. **91**, 84 (2018).

[2] T.H. Muster, A. Trinchi, T.A. Markley, D. Lau, P. Martin, A. Bradbury, A. Bendavid, and S. Dligatch, Electrochim. Acta **56**, 9679 (2011).

[3] S. Amemiya, A.J. Bard, F.-R.F. Fan, M. V. Mirkin, and P.R. Unwin, Annu. Rev. Anal. Chem. **1**, 95 (2008).

[4] M. V. Mirkin, W. Nogala, J. Velmurugan, and Y. Wang, Phys. Chem. Chem. Phys. **13**, 21196 (2011).

[5] P. Sun, F.O. Laforge, and M. V. Mirkin, Phys. Chem. Chem. Phys. **9**, 802 (2007).

[6] O.E. Hüsser, J. Electrochem. Soc. **136**, 3222 (1989).

[7] C.G. Zoski, J. Electrochem. Soc. **163**, H3088 (2016).

[8] Y. Takahashi, A.I. Shevchuk, P. Novak, Y. Murakami, H. Shiku, Y.E. Korchev, and T. Matsue, J. Am. Chem. Soc. **132**, 10118 (2010).

[9] B. Gollas, P.N. Bartlett, and G. Denuault, Anal. Chem. **72**, 349 (2000).

[10] T.H. Treutler and G. Wittstock, Electrochim. Acta **48**, 2923 (2003).

[11] R.L. Calhoun and A.J. Bard, Grahame Award Symp. Phys. Anal. Electrochem. **35**, 39 (2011).

[12] R.J. Fasching, Y. Tao, and F.B. Prinz, Sensors Actuators, B Chem. **108**, 964 (2005).

[13] A. Lesch, D. Momotenko, F. Cortés-Salazar, I. Wirth, U.M. Tefashe, F. Meiners, B. Vaske, H.H. Girault, and G. Wittstock, J. Electroanal. Chem. **666**, 52 (2012).

[14] A. Lesch, D. Momotenko, F. Cortés-Salazar, F. Roelfs, H.H. Girault, and G. Wittstock, Electrochim. Acta **110**, 30 (2013).

[15] M.P. Nagale and I. Fritsch, Anal. Chem. **70**, 2902 (1998).

[16] D.J. Comstock, J.W. Elam, M.J. Pellin, and M.C. Hersam, Anal. Chem. **82**, 1270 (2010).

[17] E.J. Candes and M.B. Wakin, IEEE Signal Process. Mag. **25**, 21 (2008).

[18] M.A. Davenport, M.F. Duarte, Y.C. Eldar, and G. Kutyniok, Compress. Sens. Theory Appl. 1 (2009).

[19] D. Momotenko, J.C. Byers, K. McKelvey, M. Kang, and P.R. Unwin, ACS Nano **9**, 8942 (2015).

[20] B.D.B. Aaronson, J.C. Byers, A.W. Colburn, K. McKelvey, and P.R. Unwin, Anal. Chem. **87**, 4129 (2015).

[21] J.M. Gregoire, C. Xiang, X. Liu, M. Marcin, and J. Jin, Rev. Sci. Instrum. **84**, (2013).

[22] G.D. O'Neil, H.W. Kuo, D.N. Lomax, J. Wright, and D. V. Esposito, Anal. Chem. **90**, 11531 (2018).

[23] D. V. Esposito, J.B. Baxter, J. John, N.S. Lewis, T.P. Moffat, T. Ogitsu, G.D. O'Neil, T.A. Pham, A.A. Talin, J.M. Velazquez, and B.C. Wood, Energy Environ. Sci. **8**, 2863 (2015).

[24] K.R. Wehmeyer, M.R. Deakin, and R.M. Wightman, Anal. Chem. **57**, 1913 (1985).

[25] A. Lesch, B. Vaske, F. Meiners, D. Momotenko, F. Cortés-Salazar, H.H. Girault, and G. Wittstock, Angew. Chemie - Int. Ed. **51**, 10413 (2012).

[26] A.J. Bard and L.R. Faulkner, *Electrochemical Methods Fundamentals and Applications*, 2nd

ed. (Wiley, 2001).

[27] J. Kwak and A.J. Bard, Anal. Chem. **61**, 1221 (1989).

[28] M.A. Mezour, M. Morin, and J. Mauzeroll, Anal. Chem. **83**, 2378 (2011).

[29] T.J. Cardwell, J. Mocak, J.H. Santos, and A.M. Bond, Analyst **121**, 357 (1996).

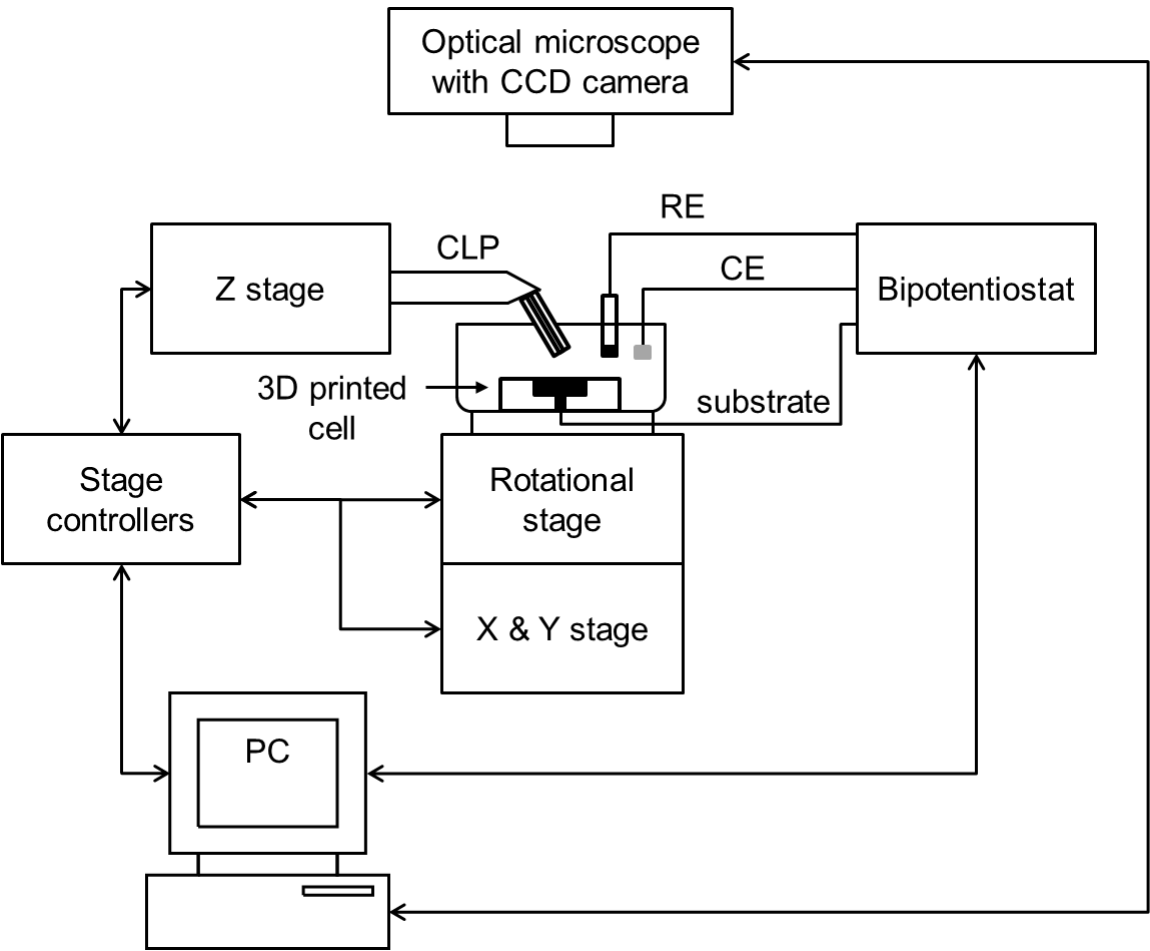
Optical microscope with CCD camera
RE
CLP
CE
Z stage
Bipotentiostat
3D printed cell
substrate
Stage controllers
Rotational stage
X & Y stage
PC

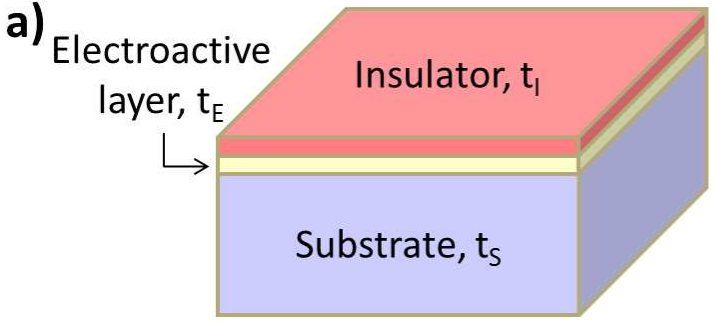
a)
Electroactive layer, t_E
Insulator, t_I
Substrate, t_S

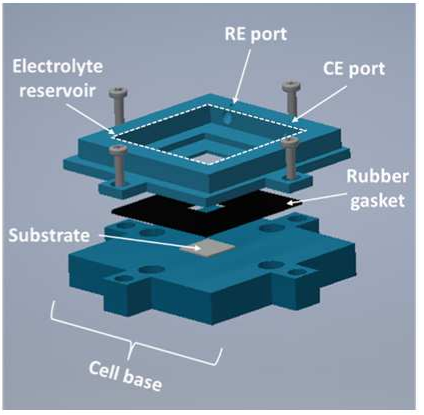
c)
RE port
Electrolyte reservoir
CE port
Rubber gasket
Substrate
Cell base

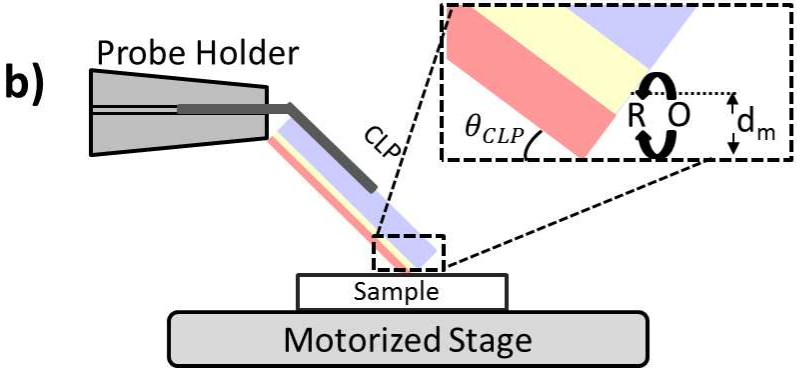
b)
Probe Holder
CLP
θ_{CLP}
R
O
d_m
Sample
Motorized Stage

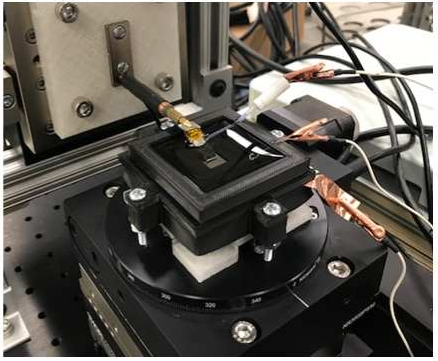
d)

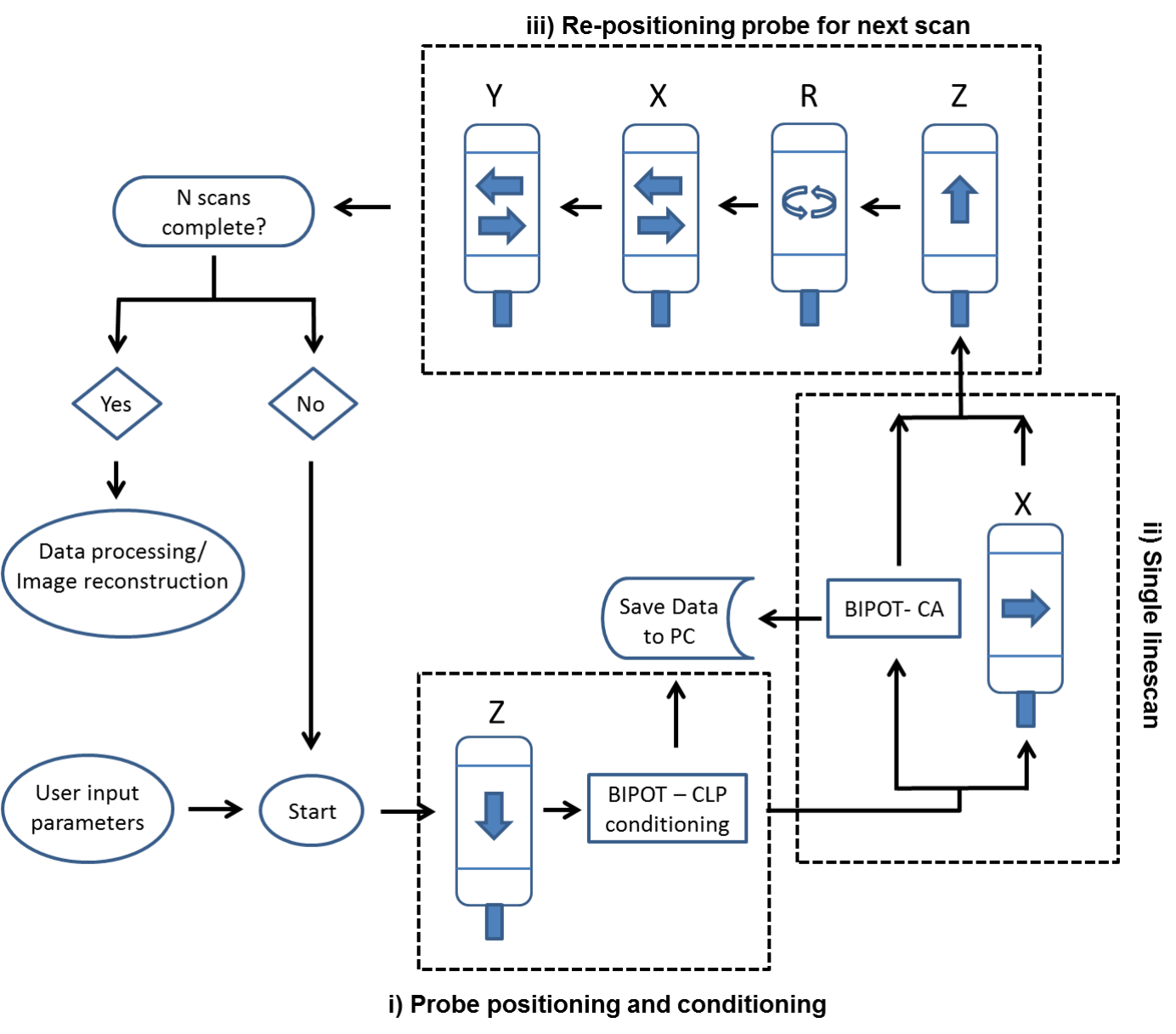
iii) Re-positioning probe for next scan
Y
X
R
Z
N scans complete?
Yes
No
Data processing/ Image reconstruction
User input parameters
Start
Z
BIPOT – CLP conditioning
Save Data to PC
BIPOT- CA
X
ii) Single linescan
i) Probe positioning and conditioning

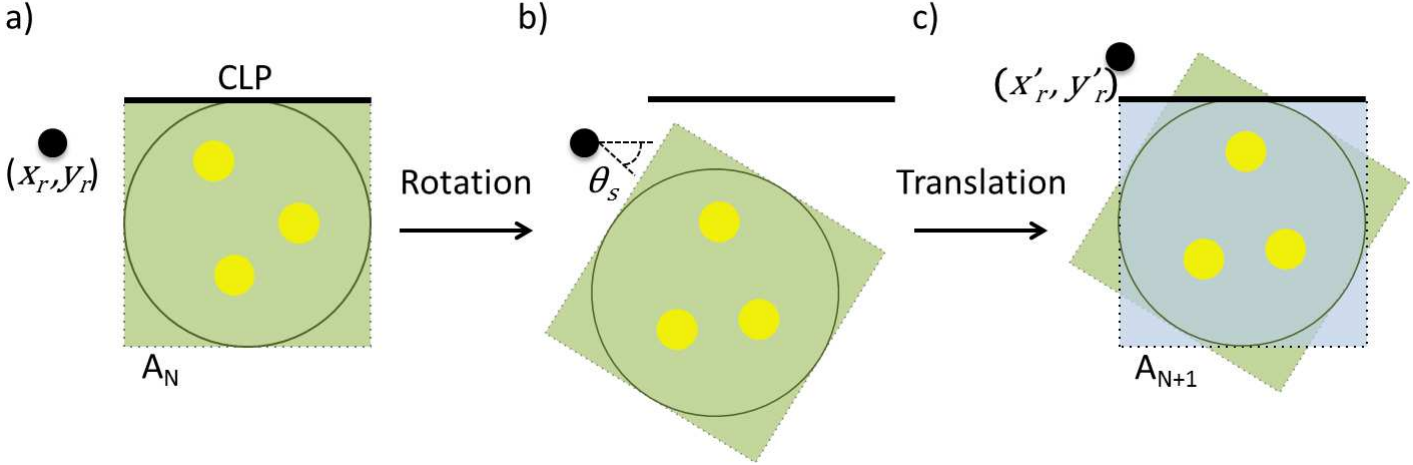
a)
CLP
(x_r, y_r)
A_N
Rotation
b)
θ_s
Translation
c)
(x'_r, y'_r)
A_{N+1}

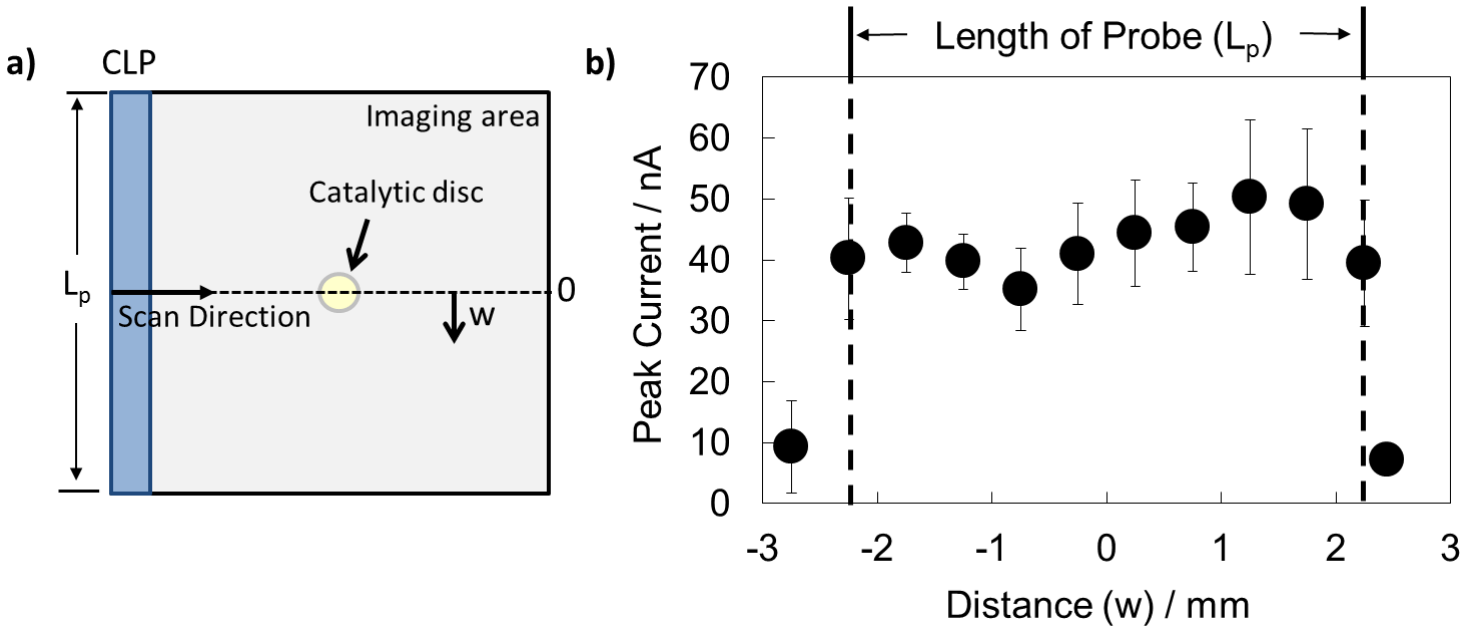
a)
CLP
Imaging area
Catalytic disc
L_p
Scan Direction
w
0
b)
Length of Probe (L_p)
Peak Current / nA
70
60
50
40
30
20
10
0
-3
-2
-1
0
1
2
3
Distance (w) / mm

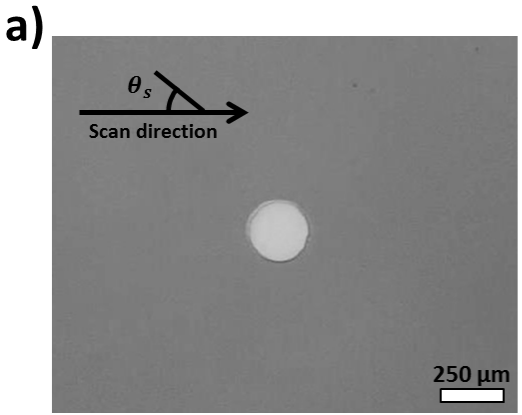
a)
θ_s
Scan direction
250 µm

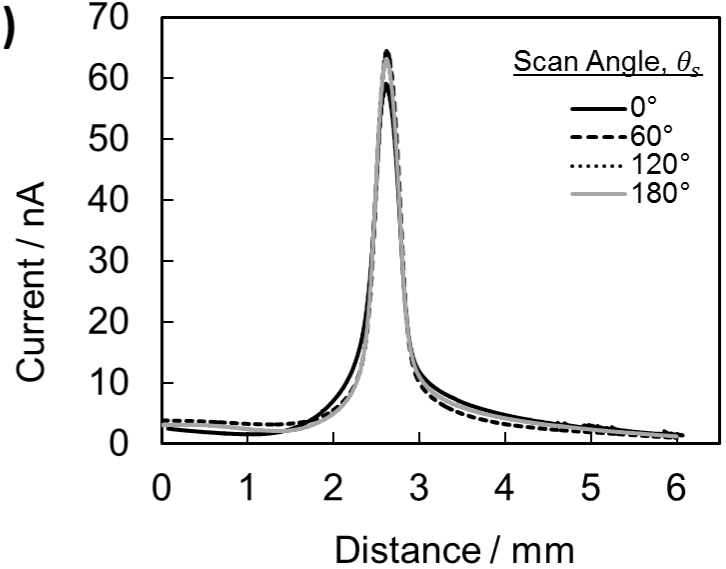
b)
Scan Angle, θ_s
0°
60°
120°
180°
Current / nA
Distance / mm
0
10
20
30
40
50
60
70
0
1
2
3
4
5
6

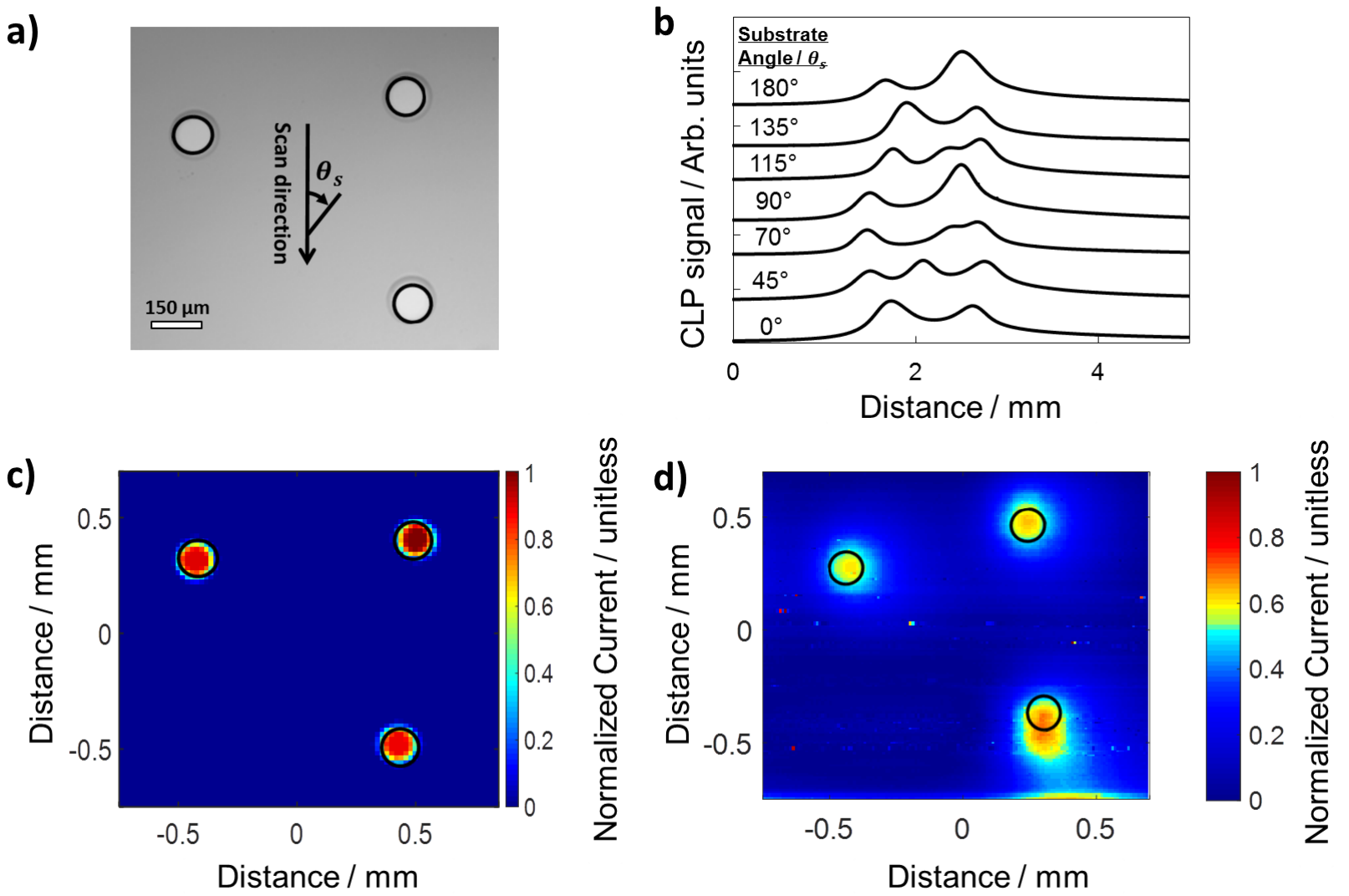
a)
Scan direction
θ_s
150 µm
b
Substrate
Angle / θ_s
180°
135°
115°
90°
70°
45°
0°
CLP signal / Arb. units
0
2
4
Distance / mm
c)
Distance / mm
0.5
0
-0.5
-0.5
0
0.5
Distance / mm
1
0.8
0.6
0.4
0.2
0
Normalized Current / unitless
d)
Distance / mm
0.5
0
-0.5
-0.5
0
0.5
Distance / mm
1
0.8
0.6
0.4
0.2
0
Normalized Current / unitless

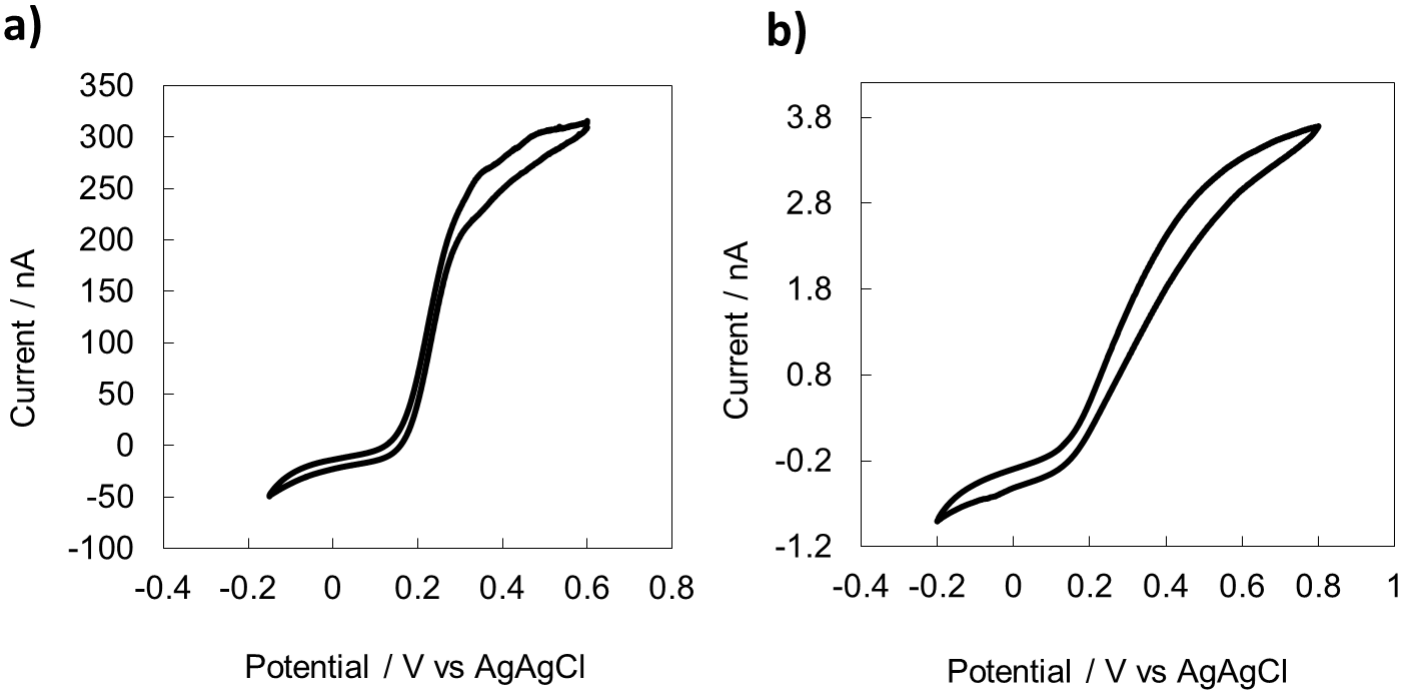
a)
350
300
250
200
150
100
50
0
-50
-100
Current / nA
-0.4
-0.2
0
0.2
0.4
0.6
0.8
Potential / V vs AgAgCl
b)
3.8
2.8
1.8
0.8
-0.2
-1.2
Current / nA
-0.4
-0.2
0
0.2
0.4
0.6
0.8
1
Potential / V vs AgAgCl

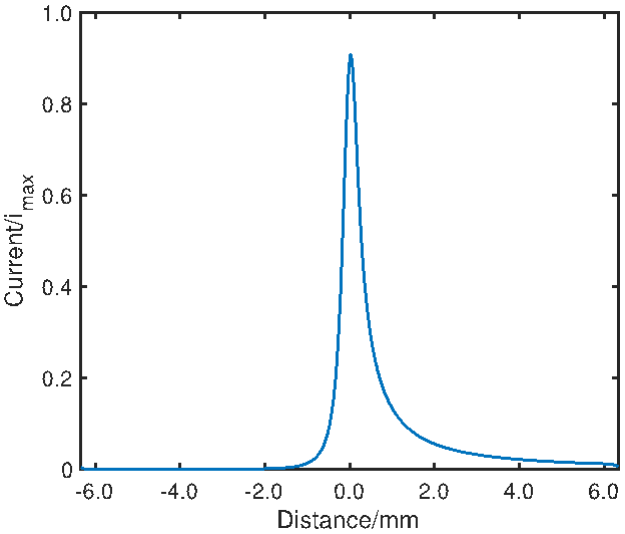
1.0
0.8
0.6
0.4
0.2
0
Current/i_max
-6.0
-4.0
-2.0
0.0
2.0
4.0
6.0
Distance/mm

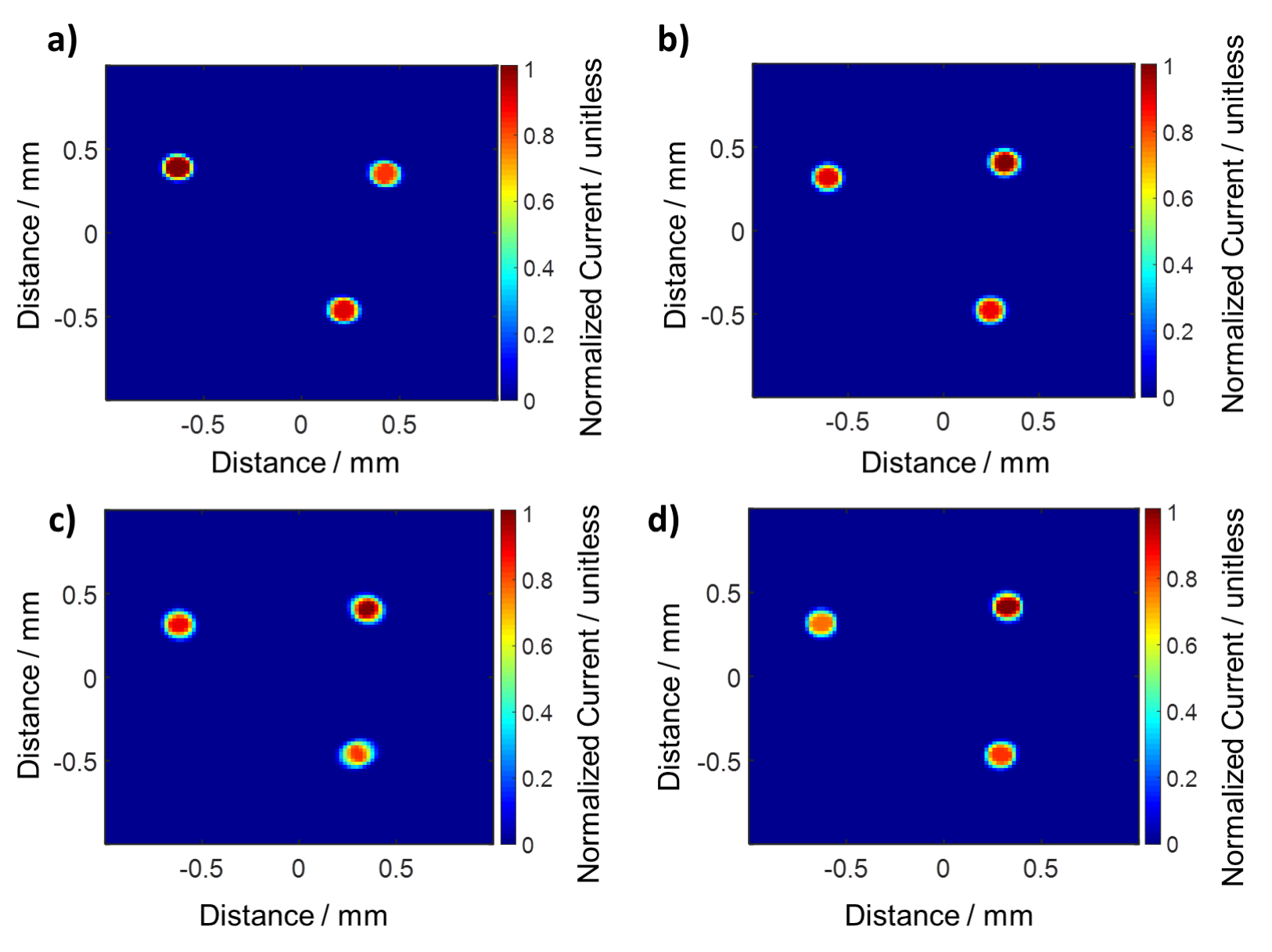
a)
b)
c)
d)
Distance / mm
Normalized Current / unitless
0.5
0
-0.5
1
0.8
0.6
0.4
0.2
0